

Chiral Assemblies of Achiral Rigid-Flexible Molecules at the Air/Water Interface Induced by Silver(I) Coordination

Libin Liu,^{*,[a], [b]} Tianduo Li,^[a] and Myongsoo Lee^{*,[b]}

Chiral films are obtained from achiral rigid-flexible molecules. Due to hydrogen bonding and steric constraints, these molecules can self-assemble into chiral assemblies at the air/water interface upon compression. When the molecules are spread on a subphase containing AgNO₃, they form a stable monolayer through coordination with Ag^I ions, as confirmed by surface

pressure–area isotherms, UV/Vis and FTIR spectroscopy, and AFM. More interestingly, macroscopic chirality was detected in the Ag^I-coordinated films by circular dichroism measurements. The formation mechanisms of the two kinds of chiral films are briefly discussed.

1. Introduction

Recently, increasing attention has been paid to the chirality of supramolecular systems, because of their important roles in both life and materials science.^[1] Generally, the chirality of supramolecular systems can be generated through the assembly of chiral molecules^[2] or through interactions between achiral molecules, such as π - π stacking, hydrogen bonding, electrostatic interactions, and coordination, yielding a chiral aggregate.^[3,4] In the latter case, construction of chiral supramolecular assemblies from achiral components is interesting, since macroscopic chirality could be realized by a stereoregular arrangement without any chiral auxiliaries, whereby molecular configuration plays a crucial role.^[5] Studies on molecular design and formation mechanism of chirality are thus important for constructing novel and controllable superhelices, especially from achiral molecules.

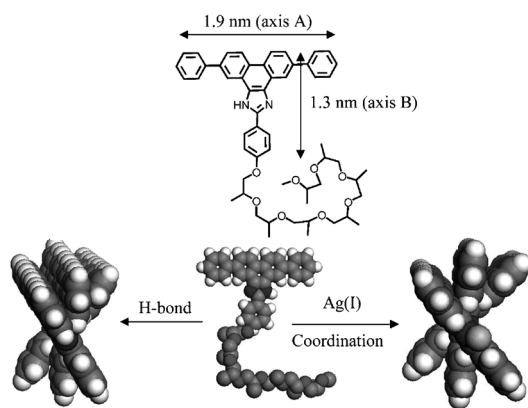
Previously, we reported that chiral assemblies could be obtained from a series of achiral rigid-flexible molecules at the air/water interface upon compression.^[6c] Hydrogen bonding and steric constraints are responsible for the macroscopic chirality. Now we extend our investigations to a new compound which contains a short benzene-ring backbone (Scheme 1) and

investigate the surface behavior of its Ag^I-coordinated film. Due to hydrogen bonding and steric constraints, this compound can self-assemble into chiral assemblies at the air/water interface upon compression. Furthermore, when the compound was spread on a subphase containing AgNO₃, the molecules formed a stable monolayer through coordination with Ag^I ions. More interestingly, macroscopic chirality was detected in the Ag^I-coordinated films.

Experimental Section

Materials: The amphiphilic rigid-flexible compound described here consists of an oligo(*p*-phenylene) conjugated rod with a poly(propylene oxide) (PPO) coil laterally attached through an imidazole linkage. The synthetic procedures and characterization are described in the Supporting Information. The resulting rigid-flexible amphiphile was characterized by ¹H and ¹³C NMR spectroscopy, elemental analysis, and matrix-assisted laser desorption ionization time-of-flight (MALDI-TOF) mass spectroscopy and shown to be in full agreement with the structure presented in Scheme 1.

Monolayer Fabrication: Langmuir isotherms at the air/water interface and Langmuir-Blodgett (LB) deposition onto a solid substrate were conducted at room temperature by using a KSV 2000 LB minitrough. A 40–120 μ L volume of dilute solution of the compound ($c < 0.5 \text{ mg mL}^{-1}$) in chloroform (HPLC grade) was deposited in 5–10 drops uniformly distributed on the water surface (Nanopure,



Scheme 1. Structure of the rigid-flexible molecule and schematics of the chiral assemblies formed from the molecules (PPO chain omitted for clarity).

[a] Dr. L. Liu, Prof. T. Li
Shandong Provincial Key Laboratory of Fine Chemicals
Shandong Institute of Light Industry
Jinan, 250353 (China)
E-mail: lbliu@spu.edu.cn

[b] Dr. L. Liu, Prof. M. Lee
Center for Supramolecular Nano-Assembly
Department of Chemistry
Seoul National University
Seoul, 151-747 (Korea)
E-mail: myongslee@snu.ac.kr

Supporting information for this article is available on the WWW under <http://dx.doi.org/10.1002/cphc.201100675>.

18.2 M Ω cm⁻¹) and left to evaporate and spread evenly for 30 min. The limiting cross-sectional area was determined at the steep rise in the surface pressure related to the formation of condensed monolayer. For AFM measurements, the monolayer LB films were transferred at a rate of 2 mm min⁻¹ onto silicon wafers at various surface pressures by the upstroke mode of the vertical dipping method. For UV/Vis, CD, and FTIR spectral measurements, the floating films were transferred onto quartz and ZnSe solid supports at selected surface pressure by the horizontal Langmuir–Schaefer method and by a certain number of depositions.

Highly polished [100] silicon wafers (Semiconductor Processing Co.) were cut into rectangular pieces (2×2 cm²) and sonicated in Nanopure water for 10 min to remove silicon dust. The wafers were then chemically treated with piranha solution (30% concentrated hydrogen peroxide, 70% concentrated sulfuric acid; **Caution:** hazardous solution!) for 1 h and then washed with abundant Nanopure water.

Monolayer Characterization: The LB monolayers on the silicon substrates were studied with a Nanoscope IIIa Multimode AFM. Scans were performed in the “light” tapping mode in accordance with the usual procedure adopted in our laboratory.^[7] An amplitude ratio of 0.95 and higher was employed to avoid monolayer damage.^[8] The domain topography and the surface area coverage were calculated from height histograms by bearing analysis.^[9] AFM characterization of the deposited LB films was done after drying in a desiccator for 24 h. The AFM scans were conducted at 0.5–2 Hz scanning rate. The AFM tip radii were between 20 and 35 nm, and the spring constants of these cantilevers were in the range of 40–60 N m⁻¹. UV/Vis and CD measurements on the films were performed at room temperature using UV-1650PC and JASCO J-810CD spectrophotometer, respectively. In the measurement of the CD spectra, the multilayer films were placed perpendicular to the light path and rotated within the film plane to avoid polarization-dependent reflections and eliminate the possible angle dependence of the CD signal.^[10] SEM-EDX spectra were performed with a JSM 6700 F NT equipped with a Link analytical system. FTIR measurements were recorded on Equinox 55 FTIR spectrophotometer with an average of several hundred scans.

2. Results and Discussion

On the pure water surface the title compound exhibited distinct amphiphilic properties. The surface pressure–area (π – A) isotherm reveals a stable Langmuir monolayer at the air/water interface (Figure 1). A shoulder appeared at a surface pressure of 11.8 mN m⁻¹. Before and after the shoulder, the limiting cross-sectional molecular areas calculated by extrapolation of the steep rise in the surface pressure to zero level are 2.65 and 1.86 nm², respectively. The values, which are just before the shoulder on the large molecular area side and just before film collapse, are consistent with the area occupied by a molecule in the flat-on and vertical orientations, which are about 2.81 and 2.07 nm², respectively.^[11] Therefore, the shoulder in the isotherm likely indicates a transformation of the aromatic rod segment of the molecule from flat-on to vertical orientation upon compression, similar to the orientation of rigid–flexible molecules at the air/water interface demonstrated in our previous work.^[6]

When the compound was spread on a subphase containing 1×10⁻³ M AgNO₃, the shoulder in the isotherm disappeared

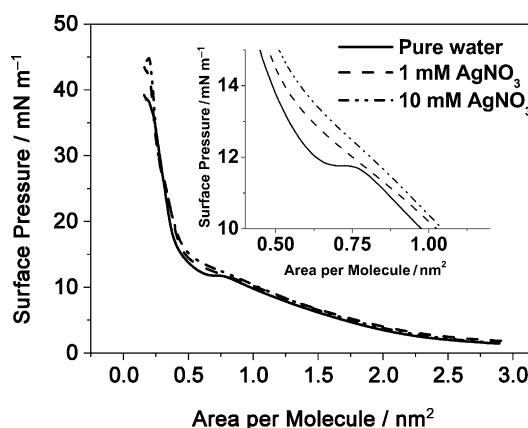


Figure 1. Surface pressure–area isotherms of the rigid–flexible molecules spread on the pure water subphase and subphase containing AgNO₃.

and the monolayer collapsed at a high surface pressure of 44 mN m⁻¹. Further addition of AgNO₃ to the subphase did not affect the isotherm significantly (Figure 1). Considering the radius of Ag^I ions to be 0.116 nm,^[12] it is reasonable to assume that the slight increase in the limiting molecular area is due to formation of an Ag^I-coordinated film.

The compound is readily soluble in CHCl₃, and displays two intense B bands at 290 and 322 nm, accompanied by one weaker Q band at 375 nm in the absorption spectrum (Figure 2a). The UV/Vis spectra of the LB films deposited from pure water surface revealed redshifts of the both B bands and Q band, indicating formation of J-aggregates in the films. For the LB films deposited from the subphase containing AgNO₃, only one B band at 295 nm and a broad Q band were ob-

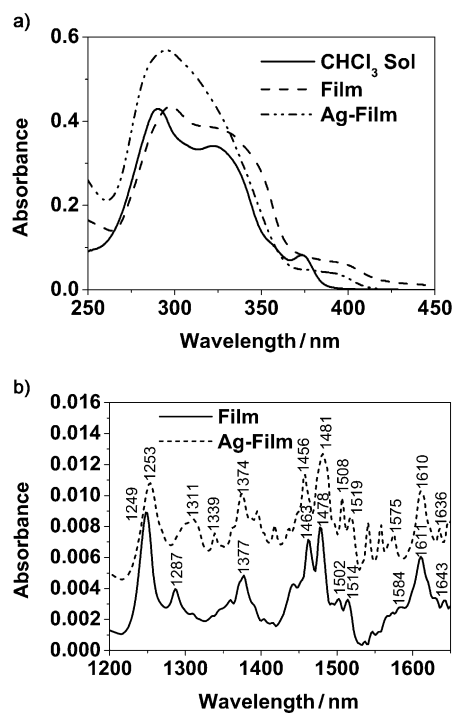


Figure 2. a) UV/Vis spectra and b) FTIR spectra of a 30-layer LB film deposited from pure water surface and aqueous AgNO₃ subphase.

served, completely different from the LB film deposited from pure water subphase, indicating that coordination of the molecules with Ag^+ occurred.

To further confirm such complex formation, the FTIR spectra of the LB films deposited from pure water and AgNO_3 subphases were measured. Figure 2b shows the main bands of the LB films deposited from pure water surface at 1643, 1611, 1584, 1514, 1502, 1478, 1463, 1377, 1287 and 1249 cm^{-1} . When the films were transferred to the AgNO_3 subphase, the IR bands changed to 1636, 1610, 1575, 1519, 1508, 1481, 1456, 1374, 1339, 1311, and 1253 cm^{-1} . The band at 1643 cm^{-1} can be assigned to the C=N vibration in the conjugated benzimidazole ring, while the bands at 1611, 1584, 1502, and 1463 cm^{-1} can be assigned to the aromatic rings. When the LB films were transferred to the AgNO_3 subphase, the C=N band shifted to 1636 cm^{-1} , while those bands assigned to aromatic rings shifted to 1610, 1575, 1508 and 1456 cm^{-1} . These spectral changes are in accordance with those reported elsewhere for imidazole ligands before and after coordination with Ag^+ .^[13] An SEM-EDX elemental analysis showed that the N:Ag molar ratio of the Ag^+ -coordinated films was approximately 2.95:1.24 (Supporting Information, Figure S2). This indicates that one Ag^+ ion was incorporated per molecule of the monolayer and the film was fully coordinated.

Atomic force microscopy (AFM) was performed on LB monolayers to further confirm the structures. The monolayer transferred from pure water surface at low surface pressure revealed smooth and uniform films. Upon compression cylinders were irregularly dispersed on the silicon wafer (Supporting Information, Figure S1). Interestingly, when the film was deposited after the shoulder (at 15 mN m^{-1}), AFM images revealed irregular ellipse-shaped structures (Figure 3a and b). Between the elliptical structures, cylinders were also present. The height of the elliptical structure is about 1.6 nm, similar to the height of the aromatic segments adopting the standing-up conformation atop the PPO layer. Further compression led to more densely packed elliptical structures (Supporting Information, Figure S1). Remarkably, the films deposited from aqueous AgNO_3 subphase at a surface pressure of 10 mN m^{-1} revealed the presence of nanoribbons (Figure 3c and d). The ribbons have an average height of 1.4 nm and average width of 13.7 nm (dimensions after correction for the tip-broadening effect).^[14] The height of the ribbons is compatible with the height of the aromatic rod segment, estimated as 1.3 nm by means of the Corey–Pauling–Koltun (CPK) model. We also performed AFM measurement on multilayers. In all cases, AFM images show full area coverage of the Langmuir–Blodgett film and a high film transfer ratio (0.8–0.9) of each layer. This indicates that the morphology of the films formed at the air/water interface is preserved upon transfer.^[15] The completely different morphology of the films obtained from the two kinds of

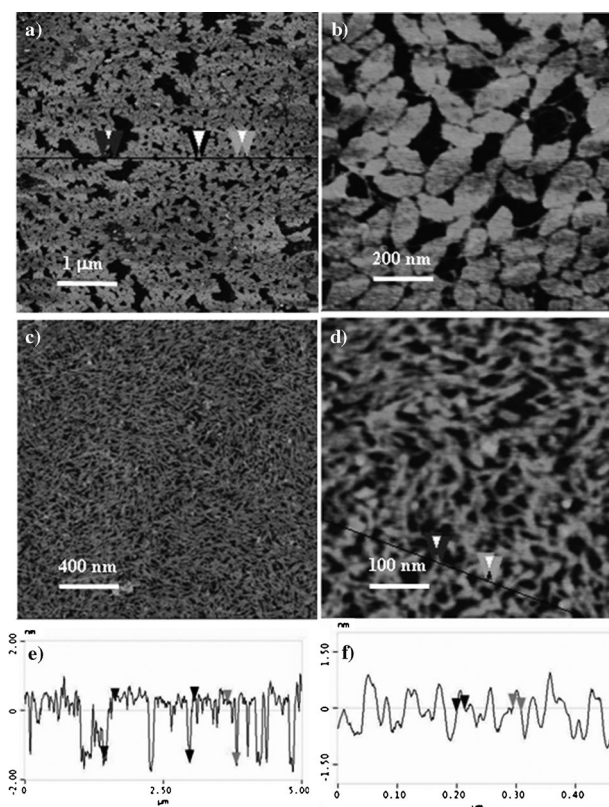


Figure 3. AFM images of the LB film deposited at a) and b) 15 mN m^{-1} with pure water as subphase; c) and d) 10 mN m^{-1} with 10 mM AgNO_3 as subphase. e) and f) Height profiles along the black lines in (a) and (d), respectively.

subphase indicates that silver coordination plays some role.

As we expected, the LB film deposited from pure water subphase showed CD signals (Figure 4a). Considering that the LB films showed two strong B bands at around 300 nm (axis A transition) and 325 nm (axis B transition), it can be suggested that exciton couplets existed in both the A and B axis transitions. Exciton coupling arises from interactions between neighboring chromophores through their locally excited states. More interestingly, in the Ag^+ -coordinated LB film the CD spectra also revealed a positive Cotton effect at 278 nm, which is close to the absorption band of the films, and thus indicates that the Cotton effect is due to the chromophores without any coupling. In addition, we also obtained opposite CD signals in

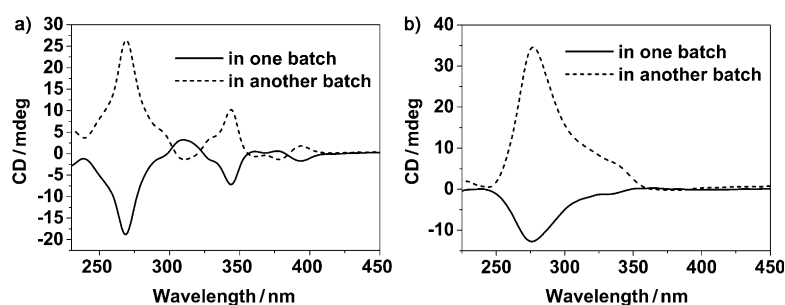


Figure 4. CD spectra of LB films deposited from pure water subphase (a) and aqueous AgNO_3 subphase (b).

different deposition batches for the two kinds of films (Figure 4).

To solely confirm that the supramolecular chirality in the LB film deposited from pure water subphase and AgNO_3 subphase really results from the packing of the molecules, and not from parasitic artifacts which originate from the interaction between macroscopic anisotropies such as birefringence and linear dichroism (LD), we measured the angle dependence of the CD spectra.^[16] The sample was placed perpendicular to the light path to avoid birefringence contributions and rotated in steps of 10° around the optical axis. The angle dependence of the CD amplitude is determined by the difference between the maximum value at 278 nm and minimum value at 350 nm for the film deposited from the AgNO_3 subphase (for the film deposited from pure water subphase the corresponding values are 270 and 310 nm), and the corresponding angle dependence of the background is determined by the difference between the values at the upper wavelength edge at 450 nm and lower edge at 250 nm, as shown in Figure 5 (see also Figure S3 in the Supporting Information). Both amplitudes can be approximated by a $\cos 2\beta$ function. The cosine function of the background is situated around 0 mdeg, while that of the sample is positively shifted to about 35 mdeg compared with that of the background for the film deposited from the AgNO_3 subphase (23 mdeg for the film deposited from pure water subphase). This is a clear indication that intrinsic chirality really exists in the LB films. Recently, Aida et al. and Meijer et al. observed LD in aligned nanofiber systems.^[16] In our case, the oriented direction of the LB film relative to the vertical axis of linearly polarized incident light was altered discontinuously within the range of 0 – 360° during the LD spectral measurements. Both kinds of films showed LD spectra (Supporting Information, Figure S4), and this indicates that LD also contributed to the observed CD spectra. For evaluating the spectral contamination of the CD by LD, the true CD intensity $[(\text{CD intensity})_{\text{true}}]$ at 269 nm and 278 nm (wavelength for maximum LD intensity) for the films deposited from pure water subphase and subphase containing AgNO_3 were calculated from the observed intensities of CD $[(\text{CD intensity})_{\text{obsd}}]$ and LD $[(\text{LD intensity})_{\text{obsd}}]$ at the same wavelength by using semi-empirical Equation (1).^[17]

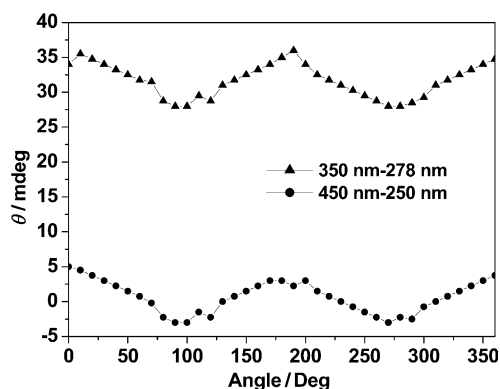


Figure 5. Angle dependence of the CD amplitude (\blacktriangle) and the background (\bullet) of the CD spectra when the LB film deposited from AgNO_3 subphase was rotated in steps of 10° within the sample plane.

$$[(\text{CD intensity})_{\text{true}}] = [(\text{CD intensity})_{\text{obsd}}] - [(\text{LD intensity})_{\text{obsd}}] \times 0.02 \quad (1)$$

The contamination of the CD by LD, as calculated by Equation (2), was evaluated to be 3.8 and 5% for the LB films deposited from pure water subphase and aqueous AgNO_3 subphase, respectively [Eq. (2)].

$$\text{Contamination [\%] of CD by LD} = 100 \times \frac{[(\text{CD intensity})_{\text{true}}] - [(\text{CD intensity})_{\text{obsd}}]}{[(\text{CD intensity})_{\text{obsd}}]} \quad (2)$$

The chirality of the LB films deposited from pure water subphase should be due to hydrogen bonding between the molecules and π - π stacking between the aromatic rod segments.^[6c] The intermolecular hydrogen bonding is in a linear fashion and such an aggregation mode is favored for aromatic rod segments with larger steric constraints to stack in a cooperative way to form chirality. When the molecules were spread on the aqueous AgNO_3 subphase, the adjacent imidazole groups in the molecule would be coordinated with Ag^+ ions. Because the aromatic rod segments are very large, the molecules are sterically overcrowded when aligned in the same plane during coordination.^[4a] Therefore, the aromatic rod segments must tilt to some extent along the polymer backbone (Scheme 1). Once a molecule starts to distort in a certain direction, the neighboring molecules would follow to form a semihelical structure at the air/water interface. This caused the chirality of the coordinated LB films. Because the chance of the backbone forming right- and left-handed helical structures is equal, our experimental results indeed revealed opposite CD signals in different batches (Figure 4). We fabricated 40 batches of LB films and found that 22 films showed positive (55%) CD signals and 18 films showed negative signals (45%) around 278 nm. Such indetermination of the chirality of the films is essentially the same as those reported for the chirality of films obtained from achiral molecules which could be due to spontaneous symmetry breaking.^[4, 18, 19]

It was recently suggested that good estimates of the amount of chiral structures could be obtained from the CD spectra of thin solid films by analyzing the wavelength dependence of the Kuhn g factor, which is also known as the ratio of the dissymmetry or anisotropy factor, and is defined as the ratio of the CD and UV/Vis absorbance signals of a sample.^[20] To compare the two different optically active LB films deposited from pure water subphase and AgNO_3 subphase, the g factor of the two kinds of films was investigated (Figure 6 and Supporting Information, Figure S5). The maximum magnitude of the g factor at the B band of the films deposited from the AgNO_3 subphase was slightly larger than that of the films deposited from pure water subphase, which is due to the larger steric constraints caused by Ag^+ ions. Although we could not deduce the exact tilting angle from our experiments, it is reasonable to suggest that the significant steric constraints resulting from the larger Ag^+ ions could promote symmetry breaking during the interfacial assembly process, because it could provide additional interspace and degrees of

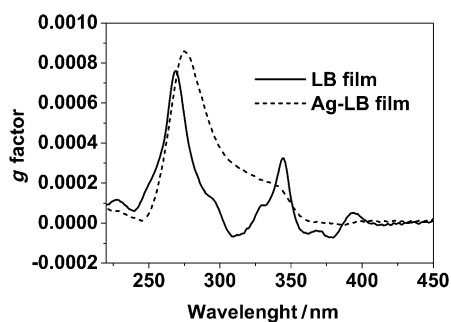


Figure 6. Kuhn g factors of the two kinds of chiral films.

the freedom for the neighboring molecules in the aggregate to cooperatively stagger each other along the axis of aggregation, producing much larger amounts of optically active supramolecules with helical conformation.

We wondered whether the chiral LB films deposited from pure water subphase could be transformed into Ag-coordinated chiral film by *ex situ* coordination. The AFM image of the monolayer showed some differences after immersion of the LB films in AgNO_3 solution, which indicates partial coordination of the films with Ag^+ in the monolayer (Supporting Information Figure S6). When a 25-layer LB film was immersed in an aqueous solution of AgNO_3 , the CD signal decreased slightly with progressing reaction. However, the CD signal did not vanish nor did the position of the peak change even after a longer reaction time (Supporting Information, Figure S7), because the coordination reaction could not be completed in the LB films due to steric hindrance.

In summary, chiral films could be obtained from an achiral rigid-flexible molecule at the air/water interface upon compression due to hydrogen bonding and steric constraints of the rod segments. By using an aqueous AgNO_3 subphase the molecules could coordinate with Ag^+ ions, as confirmed by surface pressure-area isotherms, UV/Vis and FTIR spectra, and AFM. More importantly, the Ag^+ -coordinated films showed macroscopic chirality, characterized by CD measurements, which is due to cooperative interaction of Ag^+ coordination and the steric constraints between the aromatic rod segments. This work gives important clues to the design and fabrication of chiral molecular assemblies from achiral molecules.

Acknowledgements

We gratefully acknowledge the National Natural Science Foundation of China (Grant 21176147/B060702) and the National Creative Research Initiative Program of the Korean Ministry of Science and Technology for financial support of this work.

Keywords: chirality · monolayers · rigid-flexible compounds · self-assembly · silver

- [1] a) J. M. Lehn, *Supramolecular Chemistry: Concepts and Perspectives*, Wiley-VCH, Weinheim, 1995, chap. 9; b) Special issue on supramolecular chirality: A. Scarso, J. Rebek, Jr., *Top. Curr. Chem.* **2006**, 265, 1; c) L. Liu,

- J.-K. Kim, R. Gunawidjaja, V. V. Tsukruk, M. Lee, *Langmuir* **2008**, 24, 12340; d) H.-J. Kim, J.-K. Kim, M. Lee, *Chem. Commun.* **2010**, 31, 975; e) L. Liu, H.-J. Kim, M. Lee, *Soft Matter* **2011**, 7, 91.
- [2] a) B. L. Feringa, R. A. van Delden, N. Koumura, E. M. Geertsema, *Chem. Rev.* **2000**, 100, 1789; b) V. Percec, M. R. Imam, M. Peterca, D. A. Wilson, P. A. Heiney, *J. Am. Chem. Soc.* **2009**, 131, 1294.
- [3] a) J. M. Ribó, J. Crusats, F. Sagués, J. Claret, R. Rubires, *Science* **2001**, 292, 2063; b) M. Ziegler, A. V. Davis, D. W. Johnson, K. N. Raymond, *Angew. Chem.* **2003**, 115, 689; *Angew. Chem. Int. Ed.* **2003**, 42, 665; c) H.-J. Kim, E. Lee, M. G. Kim, M.-C. Kim, E. Sim, M. Lee, *Chem. Eur. J.* **2008**, 14, 3883; d) H.-J. Kim, T. Kim, M. Lee, *Acc. Chem. Res.* **2011**, 44, 72.
- [4] a) J. Yuan, M. Liu, *J. Am. Chem. Soc.* **2003**, 125, 5051; b) X. Huang, C. Li, S. Jiang, X. Wang, B. Zhang, M. Liu, *J. Am. Chem. Soc.* **2004**, 126, 1322.
- [5] a) M. Enomoto, A. Kishimura, T. Aida, *J. Am. Chem. Soc.* **2001**, 123, 5608; b) I. Katsuki, Y. Motoda, Y. Sunatsuki, N. Matsumoto, T. Nakashima, M. Kojima, *J. Am. Chem. Soc.* **2002**, 124, 629.
- [6] a) L. Liu, K.-S. Moon, R. Gunawidjaja, E. Lee, V. V. Tsukruk, M. Lee, *Langmuir* **2008**, 24, 3930; b) L. Liu, J.-K. Kim, M. Lee, *ChemPhysChem* **2008**, 9, 1585; c) L. Liu, D.-J. Hong, M. Lee, *Langmuir* **2009**, 25, 5061; d) L. Liu, J.-K. Kim, M. Lee, *ChemPhysChem* **2010**, 11, 706.
- [7] V. V. Tsukruk, D. H. Reneker, *Polymer* **1995**, 36, 1791.
- [8] S. N. Magonov, V. Elings, M. H. Whangbo, *Surf. Sci.* **1997**, 375, L385.
- [9] S. N. Magonov, *Surface Analysis with STM and AFM: Experimental and Theoretical Aspects of Image Analysis*, VCH, New York, 1996.
- [10] C. Spitz, S. Dähne, A. Quart, H.-W. Abraham, *J. Phys. Chem. B* **2000**, 104, 8664.
- [11] The surface area occupied by the aromatic rod segments was calculated by the Corey-Pauling-Koltun (CPK) method to be about 1.35 nm^2 in the flat-on orientation ($A_{\text{rod}\parallel}$) and 0.61 nm^2 in the vertical orientation ($A_{\text{rod}\perp}$). The surface area of PPO chains (A_{PPO}) was estimated by the area occupied by ethylene oxide chains (the methyl group would be exposed to air). The surface area of the ethylene oxide monomeric units oriented at the water surface and hydrogen-bonded with 1–3 water molecules is about $0.22\text{--}0.28 \text{ nm}^2$ (J. K. Cox, K. Yu, A. Eisenberg, R. B. Lennox, *Phys. Chem. Phys.* **1999**, 1, 4417; M. C. Fauré, P. BasserEAU, M. A. Carignano, I. Szeleifer, Y. Gallot, D. Andelman, *Eur. Phys. J. B* **1998**, 3, 365). Therefore, the surface area occupied by a molecule is calculated as $A_{\text{rod}\parallel} + A_{\text{PPO}}$ in the flat-on orientation and $A_{\text{rod}\perp} + A_{\text{PPO}}$ in the vertical orientation.
- [12] a) R. D. Shanon, C. T. Prewitt, *Acta Crystallogr.* **1969**, B25, 925; b) R. D. Shanon, *Acta Crystallogr.* **1976**, A32, 751.
- [13] a) M. Liu, G. Xu, Y. Liu, Q. Chen, *Langmuir* **2001**, 17, 427; b) H. Gong, M. Liu, *Langmuir* **2001**, 17, 6228.
- [14] P. Samorí, V. Francke, T. Mangel, K. Mullen, J. P. Rabe, *Opt. Mater.* **1998**, 9, 390.
- [15] a) K. L. Genson, D. Vaknin, O. Villacencio, D. V. McGrath, V. V. Tsukruk, *J. Phys. Chem. B* **2002**, 106, 11277; b) H. Riegler, K. Spratte, *Thin Solid Films* **1992**, 210, 9.
- [16] a) A. Tsuda, Md. A. Alam, T. Harada, T. Yamaguchi, N. Ishii, T. Aida, *Angew. Chem.* **2007**, 119, 8346; *Angew. Chem. Int. Ed.* **2007**, 46, 8198; b) M. Wolffs, S. J. George, Ž. Tomović, S. C. J. Meskers, A. P. H. J. Schenning, E. W. Meijer, *Angew. Chem.* **2007**, 119, 8351; *Angew. Chem. Int. Ed.* **2007**, 46, 8203.
- [17] a) H. Gillgren, A. Stenstam, M. Ardammar, B. Nordón, E. Sparr, S. Ulvenlund, *Langmuir* **2002**, 18, 462; b) A. Ohira, K. Okoshi, M. Fujiki, M. Kunitake, M. Naito, *Adv. Mater.* **2004**, 16, 1645.
- [18] a) R. Viswanathan, J. A. Zasadzinski, D. K. Schwartz, *Nature* **1994**, 368, 440; b) L. Zhang, Q. Lu, M. Liu, *J. Phys. Chem. B* **2003**, 107, 2565; c) P. Guo, M. Liu, *Langmuir* **2005**, 21, 3410.
- [19] a) A. Pawlik, S. Kirstein, U. De Rossi, S. Dähne, *J. Phys. Chem. B* **1997**, 101, 5646; b) H. von Berlepsch, C. Böttcher, A. Quart, C. Burger, S. Dähne, S. Kirstein, *J. Phys. Chem. B* **2000**, 104, 5255.
- [20] a) P. McPhie, *Biopolymers* **2004**, 75, 140; b) P. McPhie, *Anal. Biochem.* **2001**, 293, 109.

Received: September 3, 2011

Revised: November 15, 2011

Published online on December 21, 2011